Volume 60
Number 36
4 May 2024
Pages 4735–4862

ChemComm

Chemical Communications

rsc.li/chemcomm

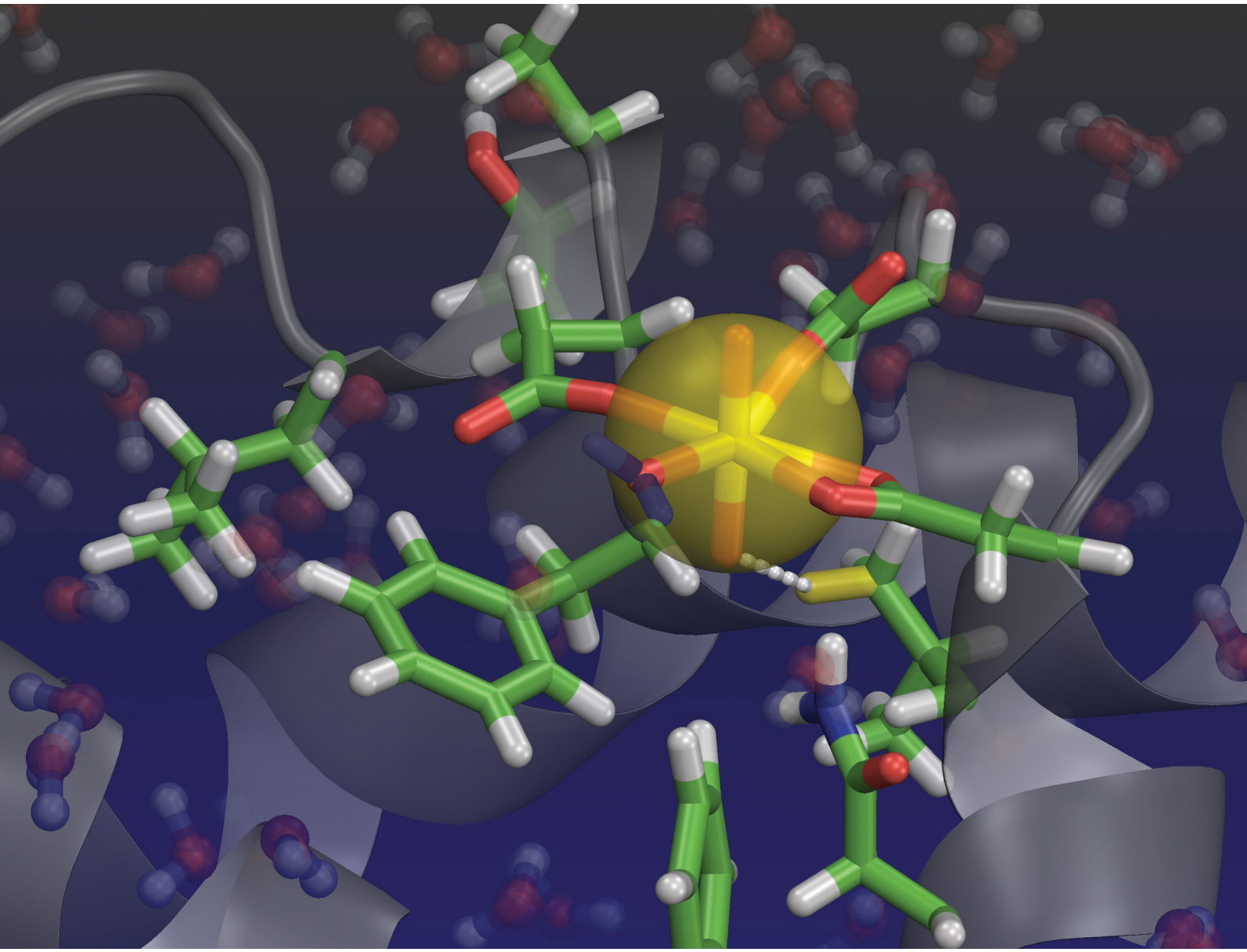

ISSN 1359-7345

ROYAL SOCIETY OF CHEMISTRY

COMMUNICATION

Satoru Tsushima *et al.*

Towards tailoring hydrophobic interaction with uranyl(VI) oxygen for C–H activation

60 YEARS ANNIVERSARY

ChemComm

COMMUNICATION

View Article Online
View Journal | View Issue

Cite this: *Chem. Commun.*, 2024, **60**, 4769

Received 5th March 2024,
Accepted 25th March 2024

DOI: 10.1039/d4cc01030b

rsc.li/chemcomm

Towards tailoring hydrophobic interaction with uranyl(VI) oxygen for C–H activation†

Satoru Tsushima, *[ab] Jérôme Kretzschmar, [a] Hideo Doi, [c] Koji Okuwaki, [c] Masashi Kaneko, [d] Yuji Mochizuki [de] and Koichiro Takao [f]

Bovine serum albumin (BSA) has a uranyl(VI) binding hotspot where uranium is tightly bound by three carboxylates. Uranyl oxygen is "soaked" into the hydrophobic core of BSA. Isopropyl hydrogen of Val is trapped near UO_2^{2+} and upon photoexcitation, C–H bond cleavage is initiated. A unique hydrophobic contact with "yl"-oxygen, as observed here, can be used to induce C–H activation.

The excited state of uranyl(VI) has a high oxidizing power of E° = +2.6 ± 0.1 V *vs.* standard hydrogen electrode (SHE), which is almost as strong as the oxidizing power of F_2.[1,2] This allows UO_2^{2+} to exhibit photocatalytic behavior toward C(sp^3)–H bonds of aliphatic compounds, which have a bond dissociation energy of nearly 100 kcal mol^{-1}.[3] A well-known example of uranyl(VI) photochemistry is the photodegradation of organic compounds in the presence of uranyl(VI) under extremely mild conditions. As such, uranium has the potential to be a sustainable catalyst. Upon photoexcitation, the "yl"-oxygen of UO_2^{2+} becomes highly reactive to induce either H-abstraction from aliphatic carbon, C=C bond cleavage,[4,5] or Ligand–Metal Charge Transfer (LMCT).[6] Uranyl(VI) photolysis can be utilized in two different ways; either to transform U(VI) into U(IV) for U recovery, or to reoxidize U(V) with air and introduce U into a catalytic cycle.[7,8] While photochemical reduction and functionalization of uranyl(VI) has often been reported in "exotic" systems, here we show that H-abstraction can be performed in a well-controlled manner in mild systems containing only ubiquitous biological substances, such as amino acids and proteins, to which direct C–H to C–C,[3,9] C–O,[10,11] or C–F[12,13] conversion can be applied.

First, we test our hypothesis that the excited uranyl(VI) aquo ion is a stronger oxidant compared to its coordination complexes, as is indicated by the fact that methanol is readily oxidized by $[UO_2^{2+}]^*$[14] while acetic acid remains intact.[15] For a uranyl-methanol mixture, a previous theoretical study suggested H-abstraction from $-CH_3$ of methanol by O_{yl} of $[UO_2^{2+}]^*$.[16] The same mechanism does not take place in the case of uranyl-acetate mixture.[15] Ligand coordination apparently downgrades the oxidizing power of $[UO_2^{2+}]^*$. On the other hand, several coordination complexes of uranyl are reported to be photoreactive, such as nitrates,[9,17,18] $[UO_2(NO_3)_2(Ph_2phen)]$,[19] and $[UO_2(OPMe_3)_4]^{2+}$.[20] We have also recently discovered that photoexcited $[UO_2(CO_3)_3]^{4-}$, which has significantly weaker oxidizing power than photoexcited $[UO_2(H_2O)_5]^{2+}$, is capable of abstracting H from BH_4^-.[21] Peptides[22,23] and proteins[24,25] are also known to be degraded by $[UO_2^{2+}]^*$. We first used quantum chemical calculations to theoretically estimate the reduction potentials of uranyl(VI) coordination complexes with the aim of confirming our hypothesis that ligand coordination reduces the oxidizing power of $[UO_2^{2+}]^*$. We followed a protocol of previous studies[26–28] for calculating reduction potentials of U(VI)/U(V) pairs and extended the calculations to include excited states. Details of the calculations are given in the ESI.† The CAM-B3LYP functional with the aug-cc-PVTZ basis set on H, C, and O as well as the small-core effective core potential (ECP) on U[29] and the CPCM solvation model in combination with Pauling's ionic radius were found to give reasonable agreement with experimental values after including spin–orbit corrections. The reduction potentials were estimated to be −0.082 and +2.478 V for $[UO_2(H_2O)_5]^{2+/+}$ and $[UO_2(H_2O)_5]^{2+*/+}$ couples, respectively. The corresponding experimental values are +0.088[30] and +2.60 V,[2] respectively. Using the same level of theory, we extended the calculation to the acetate (Ac) complexes $[UO_2(Ac)(H_2O)_3]^{0/-1}$ as well as to $[UO_2(Ac)(H_2O)_3]^{0*/-1}$ couples and obtained reduction potentials

[a] *Institute of Resource Ecology, Helmholtz–Zentrum Dresden–Rossendorf (HZDR), Dresden, 01328, Germany. E-mail: s.tsushima@hzdr.de*
[b] *International Research Frontiers Initiative (IRFI), Institute of Innovative Research, Tokyo Institute of Technology, Tokyo, 152-8550, Japan*
[c] *Department of Chemistry and Research Center for Smart Molecules, Rikkyo University, Tokyo, 171–8501, Japan*
[d] *Department of Chemistry, Osaka University, Osaka, 560-0043, Japan*
[e] *Institute of Industrial Science, The University of Tokyo, Tokyo, 153-8505, Japan*
[f] *Laboratory for Zero-Carbon Energy, Institute of Innovative Research, Tokyo Institute of Technology, Tokyo, 152-8550, Japan*

† Electronic supplementary information (ESI) available. See DOI: https://doi.org/10.1039/d4cc01030b

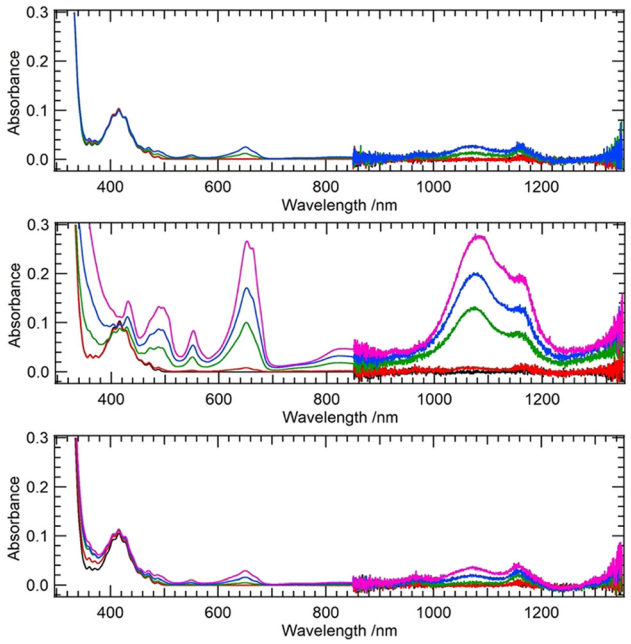

Fig. 1 Time-dependent UV-Vis-NIR spectra of 10 mM uranyl(VI) mixtures with 90.4 mM Gly (top), Val (middle), and Phe (bottom) under illumination of 365 nm light. Before illumination (black), 60 s (red), 360 s (green), 600 s (blue), and 900 s (pink) after illumination.

of −0.397 and +2.228 V, respectively. The latter value is significantly lower than that of an aquo complex redox couple. This suggests that coordination of the carboxyl group does indeed reduce the oxidizing power of UO_2^{2+} and that excited uranyl(VI) becomes a milder oxidant when coordinated by carboxyl groups. On the other hand, there are clear examples of peptides[22,23] and proteins[24,25] being degraded by $[UO_2^{2+}]^*$. Therefore our first question is whether amino acids alone have the ability to photochemically reduce uranyl(VI) carboxylate. Using a 365 nm light source, we illuminated aqueous uranyl(VI) solutions containing excess Gly, Val, or Phe, and measured time-dependent UV-Vis-NIR spectra (Fig. 1).

Among the three amino acids studied, Val undergoes the fastest photodegradation with U(VI) reduction to U(IV), while Gly and Phe are only slightly photoreactive. Gaseous by-products of the photodegradation of the U(VI)–Val system were CO_2 and H_2 (Shimadzu, GC-2014), although we could not quantify their yields. Nevertheless, it strongly suggests an H-abstraction mechanism involving aliphatic CH_3. The aliphatic amino acid Val seems to act as an effective reductant, while CH_2 from the backbone may also partially contribute to H-abstraction. However, the latter mechanism involving the backbone is likely to be difficult in the case of a peptide or protein due to steric hindrance. Therefore, we believe that the latter mechanism can only occur with amino acids and not with proteins and peptides. On the other hand, H-abstraction from protein side chains by $[UO_2^{2+}]^*$ is likely to occur provided that O_{yl} is in a hydrophobic environment within the protein. UO_2^{2+} is known to interact with metalloproteins,[24,31,32] but it is usually bound to carboxyl groups of Asp or Glu, which are in a hydrophilic environment, and U-protein remains photoinactive.

Bovine serum albumin (BSA) has a high affinity UO_2^{2+} binding site which undergoes site-specific photocleavage.[24] To obtain a clue about its photoreactivity and its relation to molecular conformation, classical molecular dynamics (MD) simulations of UO_2^{2+}-bound BSA were performed, and the MD trajectory was used to analyze the mechanism leading to site-specific photocleavage. For uranyl(VI) MD simulations, although novel 12-6-4 force fields have recently been developed by Guilbaud *et al.*[34] and have been shown to have excellent performance, we used the conventional 12-6 FF (see ESI† for details) for consistency with our previous MD-FMO work on uranyl(VI).[33] The validity of 12-6 FF in biological systems has been tested in several recent studies.[35–37] Since previous studies suggested that photocleavage of UO_2^{2+}-bound BSA occurs at Val^{314}–Cys^{315},[24] the MD simulation was performed by first aligning UO_2^{2+} in the vicinity of these residues. The simulation converged to a conformation in which uranyl(VI) is coordinated by three carboxyl groups from Asp^{307}, Asp^{311}, Asp^{313}, and additionally with a water (Fig. 2). In addition, O_{yl} is H-bonded to the side chains of Phe^{308}, Val^{314}, Phe^{325}, and occasionally to Asn^{317}. Ultimately, this O_{yl} is soaked into the hydrophobic core of the protein. On the other hand, O_{yl} at the opposite end remains in a hydrophilic environment and in loose contact with bulk water, as is generally the case for O_{yl} in water.[27] The formation of an H-bond between O_{yl} and Val^{314} confirms the experimental finding that illumination of uranyl(VI)-bound BSA leads to cleavage of the protein at Val^{314}–Cys^{315}.[24] Presumably, the photoexcited state of uranyl(VI) abstracts hydrogen from the isopropyl side chain of Val^{314}, leading to protein cleavage at Val^{314}–Cys^{315}. Although Val is not one of the most easily oxidized amino acids,[38] it apparently acts as an effective reductant as long as its aliphatic side chain is readily accessible to O_{yl}.

In order to investigate this point further and to have an extended view on the interactions acting between uranyl and protein residues, the structures obtained by MD simulations were additionally analyzed by the Fragment Molecular Orbital (FMO) method.[39–41] In FMO, the molecular system of interest is divided into smaller fragments and each fragment as well as fragment pair is subjected to self-consistent field calculations and to successive correlation energy calculations. The electronic structure of the whole system is then reconstructed. This procedure drastically reduces the computational cost and allows MP2 or even MP3 calculations of gigantic biomolecules such as fully hydrated proteins[42] or uranium–bound DNA.[33] By combining MD with FMO, we are able to compensate for some of the problems associated with the use of classical MD and can more accurately assess energetics involving weak interactions such as H-bonds and dispersion interactions. The inter-fragment interaction energy (IFIE) obtained by FMO has been used to evaluate interactions with uranyl(VI).[43–45] Although FMO is based on a full quantum chemical description, the input structures are obtained by classical MD. Calculating energy at the quantum chemical level using MD-based

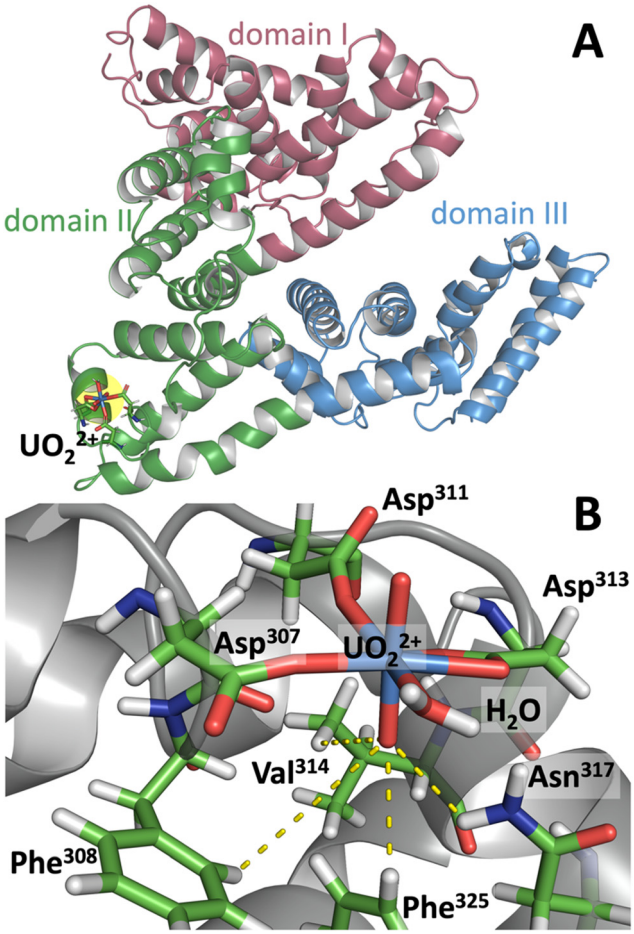

Fig. 2 Representative snapshot from the MD trajectory of UO_2^{2+}-bound BSA. Upper panel A shows the global conformation of the protein and its uranyl binding hotspot (in yellow). The lower panel B highlights the uranyl and its associated residues. Yellow dots represent hydrogen bonds involving O_{yl}.

structures can be controversial as these structures are not necessarily at the energy minima. Therefore, this approach was further strengthened by taking 100 snapshots of MD trajectories (each 1 ns from the total 100 ns simulation), all of which were subjected to FMO calculations. We used FMO in a scaled third-order Møller–Plesset perturbation scheme ($MP_{2.5}$) as reported elsewhere.[46,47] The average IFIE was calculated using 100 MD structures. Note that the IFIE is not a binding energy and refers to the interaction energy between two individual fragments (residues), thus giving us an indication of which residues are actively interacting with each other.

In Fig. 3, representative structures of BSA with and without UO_2^{2+} from MD simulations are superimposed. The two structures overlap well with each other, and there is little conformational change upon uranyl binding as far as the vicinity of the uranyl-biding site is concerned. Three Asp side chains also remain essentially in the same position and are only slightly tilted to adapt to uranyl binding. This implies that BSA can bind uranyl with little energetic cost to protein stability. This is also evident from the fact that the secondary structure of BSA

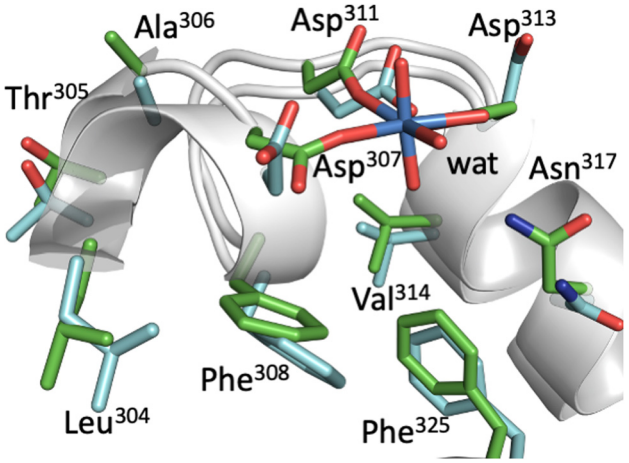

Fig. 3 Overlay of representative structures of BSA with (light green) and without (light blue) uranyl(VI). The side chains of the uranyl-interacting residues are highlighted as sticks, while the secondary structures of the protein are shown as ribbons.

remains essentially the same even after uranyl(VI) binding. On the other hand, analysis of the IFIE from FMO calculations (Table 1) shows that uranyl(VI) is not only captured by three Asp, but that there are also attractive interactions between uranyl(VI) and other side chains. These residues include Leu^{304}, Thr^{305}, Ala^{306}, Phe^{308}, and Val^{314}, most of which have hydrophobic side chains. For Val^{314}, although the average IFIE is a positive value (*i.e.*, the interaction is repulsive), the actual value at each time step varies from −20.9 to +20.2 kcal mol^{-1}, reflecting the dynamic fluctuation of the UO_2^{2+}–Val distance from 2.23 to 4.61 Å. Only when the UO_2^{2+}–Val distance is close does the interaction becomes attractive. We observed so-called "Asn flipping" during the simulation, which resulted in a large standard deviation of the IFIE for Asn^{317}. However, such behavior at atomic resolution is well known[48] and is thought to be a computational artifact. Therefore, we do not take the interaction with Asn seriously.

In summary, BSA has a binding hot spot where uranyl(VI) ions can be accommodated with high affinity. At this binding site, UO_2^{2+} is coordinated by three Asp in its equatorial shell

Table 1 Inter-fragment interaction energy (IFIE) between uranyl(VI) and major residues in its vicinity as obtained by FMO calculations at the $MP_{2.5}$ level as well as associated inter-fragment distances. Mean values from 100 structures as well as standard deviations are shown

	Distance (Å)		IFIE (kcal mol^{-1})	
	Mean	s.d.	Mean	s.d.
Leu^{304}	8.79	0.73	−9.6	1.4
Thr^{305}	7.82	0.50	−10.8	2.1
Ala^{306}	7.65	0.29	−10.2	1.7
Asp^{307}	2.19	0.04	−350.1	9.9
Phe^{308}	2.79	0.19	−26.0	13.2
Asp^{311}	2.20	0.05	−327.3	12.9
Asp^{313}	2.24	0.06	−350.3	25.0
Val^{314}	3.26	0.49	+4.8	8.6
Asn^{317}	3.61	0.77	−8.6	42.0
Phe^{325}	3.29	0.53	−6.5	1.7

and additionally captured by hydrophobic side chains. Upon photoexcitation of UO_2^{2+}, Val^{314} residing in its vicinity is oxidized by $[UO_2^{2+}]^*$ and BSA is cleaved (proteolysis). Apparently, such a binding pattern is peculiar to UO_2^{2+}–BSA, because such site-specific photocleavage has not been reported in any other uranyl(VI) protein system. Such a unique binding pattern may be adopted in uranyl photocatalysis for C–H activation. In this regard, we have recently designed a new uranyl(VI) binding peptide that also has hydrophobic interaction with O_{yl}.[49] We are also interested in further exploring the importance and relevance of the hydrophobicity of uranyl(VI) oxygen and how it relates to the environmental impact of uranium, including possible U(VI) reduction to U(V) and its stabilization. This will be the subject of our future investigation.

This work was supported by Japan Society for the Promotion of Science (ID: JP20KK0119). MD calculations were performed at the Center for Information Services and High-Performance Computing at Technische Universität Dresden, Germany. FMO calculations were performed on the Fugaku supercomputer provided by the RIKEN Center of Computational Science, Japan, as part of the HPCI System Research Project ID hp220229. YM was supported by Rikkyo University SFR. We thank Ellen Adams (HZDR/TU Dresden) for proofreading the manuscript.

Conflicts of interest

There are no conflicts to declare.

Notes and references

1 B. E. Cowie, J. M. Purkis, J. Austin, J. B. Love and P. L. Arnold, *Chem. Rev.*, 2019, **119**, 10595.
2 N. Behera and S. Sethi, *Eur. J. Inorg. Chem.*, 2021, 95.
3 B. Maity, S. Dutta and L. Cavallo, *Chem. Soc. Rev.*, 2023, **52**, 5373.
4 S. Tsushima, V. Brendler and K. Fahmy, *Dalton Trans.*, 2010, **39**, 10953.
5 S.-B. Tang, S.-Y. Zhang, W.-J. Li, Y.-X. Jiang, Z.-X. Wang, B. Long and J. Su, *Org. Chem. Front.*, 2023, **10**, 5130.
6 S. Tsushima, C. Götz and K. Fahmy, *Chem. – Eur. J.*, 2010, **16**, 8029.
7 Z. Wang, B. Li, H. Shang, X. Dong, L. Huang, Q. Qing, C. Xu, J. Chen, H. Liu, X. Wang, X.-G. Xiong and Y. Lu, *Green Chem.*, 2022, **24**, 7092.
8 I. M. DiMucci, H. D. Root, Z. R. Jones, S. A. Kozimor, M. M. Maclnnes, J. L. Miller, V. Mocko, W. J. Oldham and B. W. Stein, *Chem. Commun.*, 2022, **58**, 10961.
9 L. Capaldo, D. Merli, M. Fagnoni and D. Ravelli, *ACS Catal.*, 2019, **9**, 3054.
10 D. Hu and X. Jiang, *Green Chem.*, 2022, **24**, 124.
11 S.-Y. Zhang, S.-B. Tang, Y.-X. Jiang, R.-Y. Zhu, Z.-X. Wang, B. Long and J. Su, *Inorg. Chem.*, 2024, **63**, 2418.
12 L. Wu, X. Cao, X. Chen, W. Fang and M. Dolg, *Angew. Chem., Int. Ed.*, 2018, **57**, 11812.
13 C.-L. Chen, H.-Y. Wang, Z.-Z. Weng, L.-S. Long, L.-S. Zheng and X.-J. Kong, *Inorg. Chem.*, 2023, **62**, 17041.
14 H. D. Burrows and S. J. Formosinho, *J. Chem. Soc., Faraday Trans.*, 1977, **73**, 201.
15 K. Müller, *et al.*, *ACS Omega*, 2019, **4**, 8167.
16 S. Tsuhsima, *Inorg. Chem.*, 2009, **48**, 4856.
17 J. G. West, T. A. Bedell and E. J. Sorensen, *Angew. Chem., Int. Ed.*, 2016, **55**, 8923–8927.
18 S. Lv, Q. Li, J.-W. Sang, J. Wang and W.-D. Zhang, *RSC Adv.*, 2023, **13**, 11929.
19 P. L. Arnold, J. M. Purkis, R. Rutkauskaite, D. Kovacs, J. B. Love and J. Austin, *ChemCatChem*, 2019, **11**, 3786.
20 T. Mashita, S. Tsushima and K. Takao, *ACS Omega*, 2019, **4**, 7194.
21 K. Takao and S. Tsushima, *Dalton Trans.*, 2018, **47**, 5149.
22 L. H. Kristensen, P. E. Nielsen, C. I. Jørgensen, B. B. Kragelund and N. E. Møllegaard, *ChemBioChem*, 2008, **9**, 2377.
23 R. L. B. Elnegaard, N. E. Møllegaard, Q. Zhang, F. Kjeldsen and T. J. D. Jørgensen, *ChemBioChem*, 2017, **18**, 1117.
24 M. R. Duff and C. V. Kumar, *Angew. Chem., Int. Ed.*, 2006, **45**, 137.
25 T. Feng, Y. Yuan, S. Zhao, L. Feng, B. Yan, M. Cao, J. Zhang, W. Sun, K. Lin and N. Wang, *Angew. Chem., Int. Ed.*, 2022, **61**, e202115886 (*Angew. Chem.*, 2022, **134**, e202115886).
26 G. A. Shamov and G. Schreckenbach, *J. Phys. Chem. A*, 2005, **109**, 10961.
27 S. Tsushima, U. Wahlgren and I. Grenthe, *J. Phys. Chem. A*, 2006, **110**, 9175.
28 K. E. Gutowski and D. A. Dixon, *J. Phys. Chem. A*, 2006, **110**, 8840.
29 A. Bergner, M. Dolg, W. Küchle, H. Stoll and H. Preuß, *Mol. Phys.*, 1993, **80**, 1431.
30 I. Grenthe, X. Gaona, A. V. Plyasunov, L. Rao, W. H. Runde, B. Grambow, R. J. M. Konings, A. L. Smith and E. E. Moore, Second Update on the Chemical Thermodynamics of Uranium, Neptunium, Plutonium, Americium and Technetium, OECD Nuclear Energy Agency Data Bank, OECD Publications, Paris, France, 2020.
31 G. Montavon, C. Apostolidis, F. Bruchertseifer, U. Repinc and A. Morgenstern, *J. Inorg. Biochem.*, 2009, **103**, 1609.
32 C. Basset, O. Averseng, P.-J. Ferron, N. Richaud, A. Hagege, O. Pible and C. Vidaud, *Chem. Res. Toxicol.*, 2013, **26**, 645.
33 A. Rossberg, T. Abe, K. Okuwaki, A. Barkleit, K. Fukuzawa, T. Nakano, Y. Mochizuki and S. Tsushima, *Chem. Commun.*, 2019, **55**, 2015.
34 D. M. Martinez, D. Guillaumont and P. Guilbaud, *J. Chem. Inf. Model.*, 2022, **62**, 2432.
35 S. O. Odoh, G. D. Bondarevsky, J. Karpus, Q. Cui, C. He, R. Spezia and L. Gagliardi, *J. Am. Chem. Soc.*, 2014, **50**, 17484–17494.
36 L. Li, W. Ma, S. Shen, H. Huang, Y. Bai and H. Liu, *ACS Appl. Mater. Interfaces*, 2016, **8**, 31032–31041.
37 T. Lan, H. Wang, J. Liao, Y. Yang, Z. Chai, N. Liu and D. Wang, *Environ. Sci. Technol.*, 2016, **50**, 11121–11128.
38 J. R. Milligan, J. A. Aguilera, A. Ly, N. Q. Tran, O. Hoang and J. F. Ward, *Nucleic Acids Res.*, 2003, **31**, 6258.
39 D. G. Fedorov, T. Nagata and K. Kitaura, *Phys. Chem. Chem. Phys.*, 2012, **14**, 7562.
40 S. Tanaka, Y. Mochuzuki, Y. Komeiji, Y. Okiyama and K. Fukuzawa, *Phys. Chem. Chem. Phys.*, 2014, **16**, 10310–10344.
41 K. Fukuzawa and S. Tanaka, *Curr. Opin. Struct. Biol.*, 2022, **72**, 127.
42 B. Drobot, M. Schmidt, Y. Mochizuki, T. Abe, K. Okuwaki, F. Brulfert, S. Falke, S. A. Samsonov, Y. Komeiji, C. Betzel, T. Stumpf, J. Raff and S. Tsushima, *Phys. Chem. Chem. Phys.*, 2019, **21**, 21213.
43 T. Tokiwa, S. Nakano, Y. Yamamoto, T. Ishikawa, S. Ito, V. Sladek, K. Fukuzawa, Y. Mochizuki, H. Tokiwa, F. Misaizu and Y. Shigeta, *J. Chem. Inf. Model.*, 2019, **59**, 25.
44 K. Takaba, C. Watanabe, A. Tokuhisa, Y. Akinaga, B. Ma, R. Kanada, M. Araki, Y. Okuno, Y. Kawashima, H. Moriwaki, N. Kawashita, T. Honma, K. Fukuzawa and S. Tanaka, *J. Comput. Chem.*, 2022, **43**, 1362.
45 S. Matsuoka, K. Sakakura, Y. Akinaga, K. Akisawa, K. Okuwaki, H. Doi and Y. Mochizuki, *J. Comput. Chem.*, 2024, **45**, 898.
46 M. Pitonak, P. Neogrady, J. Cerny, S. Grimme and P. Hobza, *Chem. Phys. Chem.*, 2009, **10**, 282.
47 K. Akisawa, R. Hatada, K. Okuwaki, Y. Mochizuki, K. Fukuzawa, Y. Komeiji and S. Tanaka, *RSC Adv.*, 2021, **11**, 3272.
48 W. G. Touw, R. P. Joosten and G. Vriend, *J. Mol. Biol.*, 2016, **428**, 1375.
49 S. Tsushima and K. Takao, *Phys. Chem. Chem. Phys.*, 2022, **24**, 4455.

